

Multiple-site comparisons between models of incoherent scatter radar and IRI

Shun-Rong Zhang ^{a,*}, John M. Holt ^a, Dieter K. Bilitza ^b, Tony van Eyken ^c,
Mary McCready ^d, Christine Amory-Mazaudier ^e, Shoichiro Fukao ^f, Michael Sulzer ^g

^a MIT Haystack Observatory, Off Route 40, Westford, MA 01886, USA

^b NASA Goddard Space Flight Center, Greenbelt, MD 20771, USA

^c The EISCAT Scientific Association, P.O. Box 164, SE-981 23 Kiruna, Sweden

^d SRI International, Menlo Park, CA 94025, USA

^e Centre for the Study of Earth and Planets Environments, CNRS, 94107 Saint-Maur-des-Fossés Cedex, France

^f Research Institute for Sustainable Humanosphere, Kyoto University, Uji, Kyoto 611-0011, Japan

^g Arecibo Observatory, NAIC, HC03 Box 53995, Arecibo, Puerto Rico 00612, Puerto Rico

Received 30 December 2005; received in revised form 2 March 2006; accepted 11 May 2006

Abstract

Long-term databases of multiple incoherent scatter radars (ISRs) are used to create local empirical models at seven ISR sites including, from magnetic north to south and east to west, EISCAT Svalbard Radar (Norway), Sondrestrom Radar (Greenland), EISCAT Tromsø Radars (Norway), Millstone Hill Radar (USA), St. Santin Radar (France), Shigaraki Middle and Upper atmosphere (MU) Radar (Japan) and Arecibo Radar (Puerto Rico). As local models, they can represent some features that may be smeared out in a global model, and are important complements to and validation tools for global models such as IRI. This paper presents comparisons between these ISR models and IRI for median solar activity and quiet magnetic activity conditions, with focus on daytime height variations for electron density, ion and electron temperatures.

© 2006 COSPAR. Published by Elsevier Ltd. All rights reserved.

Keywords: Ionospheric model; Incoherent scatter radar; IRI; Electron density; Ion temperature; Electron temperature

1. Introduction

Ionospheric empirical models are important tools for many research, engineering and educational efforts. The International Reference Ionosphere (IRI) (Bilitza, 2001) is an extensively used global ionospheric model. Its electron density (Ne) component was derived largely from ionosonde observations, in particular, the peak density and its height as well as the height variation at the bottomside; satellite topside sounders provided information for constructing the shape function above the F2 peak; only very

few incoherent scatter radar (ISR) profiles were taken into account. The plasma temperature component was contributed by satellite data (of course with limited height variations) and by some ISR data which, however, came from earlier observations from the 1970–80s.

As one of the most powerful ground-based instruments for probing the Earth's upper atmosphere, incoherent scatter radar directly measures ionospheric electron density Ne, electron and ion temperatures Te and Ti, and line-of-sight ion velocity over a broad height range. Long-term ISR observations provide an extremely valuable data source for addressing significant scientific issues related to ionospheric and thermospheric climatology. Since the development of incoherent scatter radars in the 1960s, long-term observational data sets have been accumulating. Based on these data, much progress has been made in

* Corresponding author. Tel.: +1 781 981 5725; fax: +1 781 981 5766.

E-mail address: shunrong@haystack.mit.edu (S.-R. Zhang).

URL: <http://madrigal.haystack.mit.edu/models/ISRModels> (S.-R. Zhang).

recent years in constructing empirical ionospheric models. Holt et al. (2002) reported local and regional models based on Millstone Hill ISR data. Zhang and Holt (2004) and Zhang et al. (2005a) reported plasma temperature climatology and model studies using Millstone Hill and St. Santin ISR observations. Doe et al. (2005) studied a 9-year database of sunlit E region electron density altitude profiles measured by the Sondrestrom ISR to model the high-latitude solar photoionization. Local models for seven ISRs, including, from magnetic north to south and east to west, EISCAT Svalbard Radar (Norway), Sondrestrom Radar (Greenland), EISCAT TromsøRadars (Norway), Millstone Hill Radar (USA), St. Santin Radar (France), Shigaraki Middle and Upper atmosphere (MU) Radar (Japan) and Arecibo Radar (Puerto Rico), have recently become available (Zhang et al., 2005b).

Local and regional models can better maintain unique features that may be easily smeared out in global models, and are important complements to and validation tools for global models. These ISR models can provide important information for IRI improvements in many aspects, such as the bottomside and topside height profiles of Ne, Te and Ti with proper height resolutions. IRI is perhaps best suited for mid-, low- and equatorial latitudes but not so well suited for high latitudes where extremely dynamic processes take place and relatively little contributed to the model. However, it is interesting to note that amongst the seven ISR local models, three (Svalbard, Sondrestrom, EISCAT TromsøRadars) are for high latitudes and one (Millstone Hill Radar) is for a subauroral area. See Fig. 1 for a map of worldwide ISR sites and available empirical models, including those described here.

In this paper, we will report a comparative study between the ISR local models and the IRI for median solar

activity and quiet magnetic activity conditions. We will present results for each of the seven ISR sites, focusing on height variations of Ne, Ti and Te during the day in equinox, summer and winter seasons. Some descriptions on the ISR data and modeling method will be given.

2. Data and modeling method

All ISR data were obtained from the Madrigal database developed at MIT Haystack Observatory. In the database, up to December 2004, the number of experiments for Svalbard Radar (operational since 1996) is over 600 experiments, for Sondrestrom Radar (operational since 1983) over 1000, for the EISCAT Tromsøradars (operational since 1981) over 1200 experiments (over 900 experiments for the UHF radar), for Millstone Hill (operational since 1960) over 1000 experiments, for St. Santin.

Radar (operational during 1963–1987) about 100 experiments, for Shigaraki Middle and Upper Atmosphere (MU) Radar (operational since 1986) about 200 experiments, and for Arecibo Radar (operational since 1963), it is over 100 experiments. Each ISR experiment covers typically 3–7 days. A calibration run can be as short as a few hours during the day for 1 day, but there were experiments for 30 days at some sites.

Information about the data selected can be found in Zhang et al. (2005b). The modeling method was also described in that paper; below we highlight only some key facts. The data for each site are binned by month and local time with 3-month and 1-h bin sizes. Assuming a piecewise-linear function for height variation in data binning, we determine linear coefficients for various height nodes. These coefficients are assumed to be linear in the solar activity index F10.7 and magnetic activity index

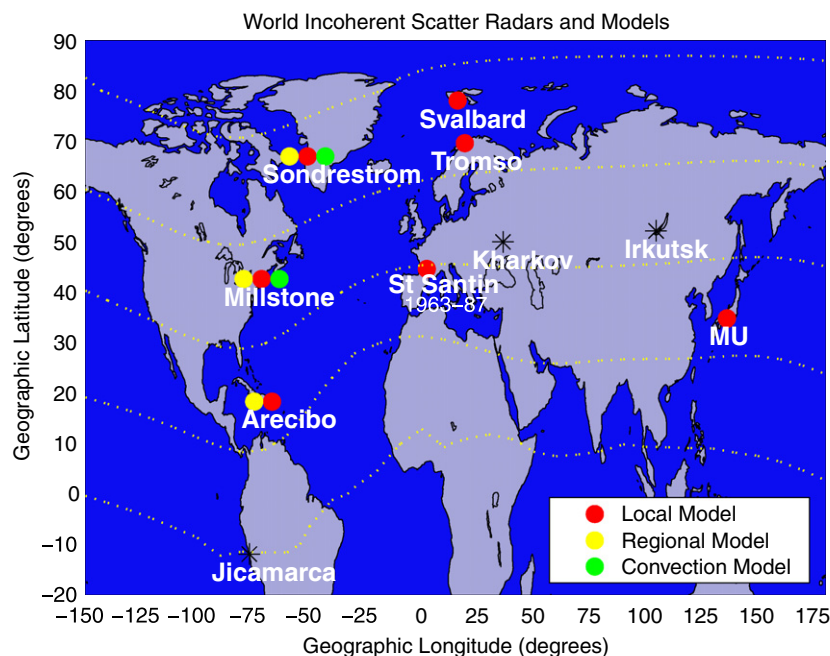


Fig. 1. Operating incoherent scatter radars and available empirical models.

3-hourly ap , where F10.7 is for the previous day and ap is for the previous 3 h. These coefficients for F10.7, ap and constant terms at each height node are determined through a least-square fit for each of the 12 months \times 24 h bins. Then they are further represented by fully analytical functions, i.e., harmonics with 12-, 6- and 4-month periodicities for seasonal changes and with 24-, 12-, 8-, and 6-h periodicities for local time changes, as well as a cubic B-spline to give twice-differentiable height variations.

3. Comparisons

Our comparisons are made for median solar activity with F10.7 = 135 units and for geomagnetically quiet conditions with daily $Ap = 15$. These conditions are applied to ISR local models, and correspond to sunspot number $Rz = 88.3$ and no magnetic storm correction that are applied to the IRI model. The IRI 2000 model Bilitza (2001) used in our comparisons is driven by such Rz value and F10.7 value for all calculations. For other IRI options, we use standard default specifications, i.e., we use the new B0 table (Bilitza et al., 2000), the CCIR foF2 coefficients and the resulting hmF2 based on its relationship with foF2, foE, M3000, etc. For T_e , two IRI models are calculated, i.e., the standard model which is based on Aeros and ISIS data, and the alternative model which is based on Intercosmos. The difference between the two IRI model starts to appear only above 450 km. With constant F10.7/ Rz , we will not examine the models' solar cycle dependency but will focus on height dependencies at noon in summer, winter and equinox.

3.1. Electron density

Fig. 2 shows comparisons for Ne between the ISR and IRI models. In general, the IRI and ISR profiles agree best in summer and worst in winter. When there exists a difference, the ISR Ne tends to be lower at heights above the F2 peak. In order to compare the profile shape, we also show the IRI Ne profile shifted and scaled in such a way that the IRI peak height and density match those on the ISR profile, and the scaling (multiplicative) factor $S = NmF2(ISR)/NmF2(IRI)$ is applied to the entire IRI Ne profile (such a scaling is equivalent to a horizontal shift of the $\log(Ne)$ profile by $\log(S)$).

At Arecibo, we can see that profile shapes from both models agree noticeably well in the topside, and are also close to each other in the lower F region (≥ 200 km). Agreement appears to be better at noon. It is noted, however, that the winter-time absolute values of Ne appears lower in the ISR model than in the IRI.

At Shigaraki, there is also generally good agreement in the profile shape. In winter when the ISR Ne is lower than the IRI Ne, the ISR profile shape indicates a slightly faster decay toward higher altitudes. Without data from below 200 km, we cannot conclusively evaluate the performance of the new IRI B0 for this lower mid-latitude site, but it

seems that the ISR Ne tends to be slightly higher than the IRI one for altitudes below the F2 peak.

At St. Santin, a typical mid-latitude site, excellent agreement is achieved in summer time or around noon in terms of the Ne magnitude and the profile shape. In winter, the ISR Ne is again lower than the IRI one.

At Millstone Hill, Ne values from both models are close in summer and equinox but the ISR Ne is lower in winter. The topside profile shapes from both models are similar with an exception at midday in winter. In the bottomside, the ISR Ne tends to be higher with a more dense F1-layer.

At Tromsø, the ISR Ne tends to be lower than the IRI Ne in the afternoon. while at noon Ne values agree better. The profile shapes above the F2 peak are generally similar with an apparent exception in winter when the Ne undergoes a decrease toward higher altitudes steeper in the ISR profile than in the IRI profile.

At Sondrestrom, the situation is similar to Millstone Hill where the topside profiles are generally similar, the bottomside Ne, especially the F1 region Ne, is higher in the ISR model than the IRI. At midday in winter, as in subauroral and high-latitude sites (Millstone Hill, Tromsø, and in Svalbard), the Ne decreases toward higher altitudes at larger rate in the ISR model than in the IRI.

At Svalbard, Ne values from both models are generally close especially at the topside, below the peak, however, the ISR model gives higher F1 region Ne. In winter, the midday Ne at and above the F2 peak is significantly lower in the ISR model than in the IRI, and below the F2 peak the ISR model gives some amount of ionization which is largely absent in the IRI.

A known issue of the current IRI Ne model is the overestimate in the topside (Bilitza and Williamson, 2000; Bilitza, 2004). This is particularly evident at high latitudes since the topside IRI model was derived from Alouette I sounder that had ground stations largely at midlatitudes in Northern Hemisphere (Bilitza, 2004). Our above results indicate that the overestimate appears to be more pronounced in winter.

3.2. Ion temperature

Results of T_i comparisons are shown in Fig. 3. Values of T_i and its height variation from ISR and IRI models agree generally very well at Arecibo, Millstone Hill and St. Santin. At Shigaraki, between 250 and 400 km within which the MU radar provides the best quality of temperature data, the models are more consistent at noon than in the afternoon. In the afternoon, the ISR model T_i is slightly higher than the IRI, and the noon-afternoon difference in T_i in IRI is not as large as in the ISR model.

At three high latitude sites, from 100 km up to 300–350 km T_i values from both models are consistent, except at Tromsø where the IRI T_i underestimates the ISR T_i . In the topside, however, the ISR T_i is lower than the IRI, This is due to the fact that the IRI model shows a steady increase with height, whereas the ISR model

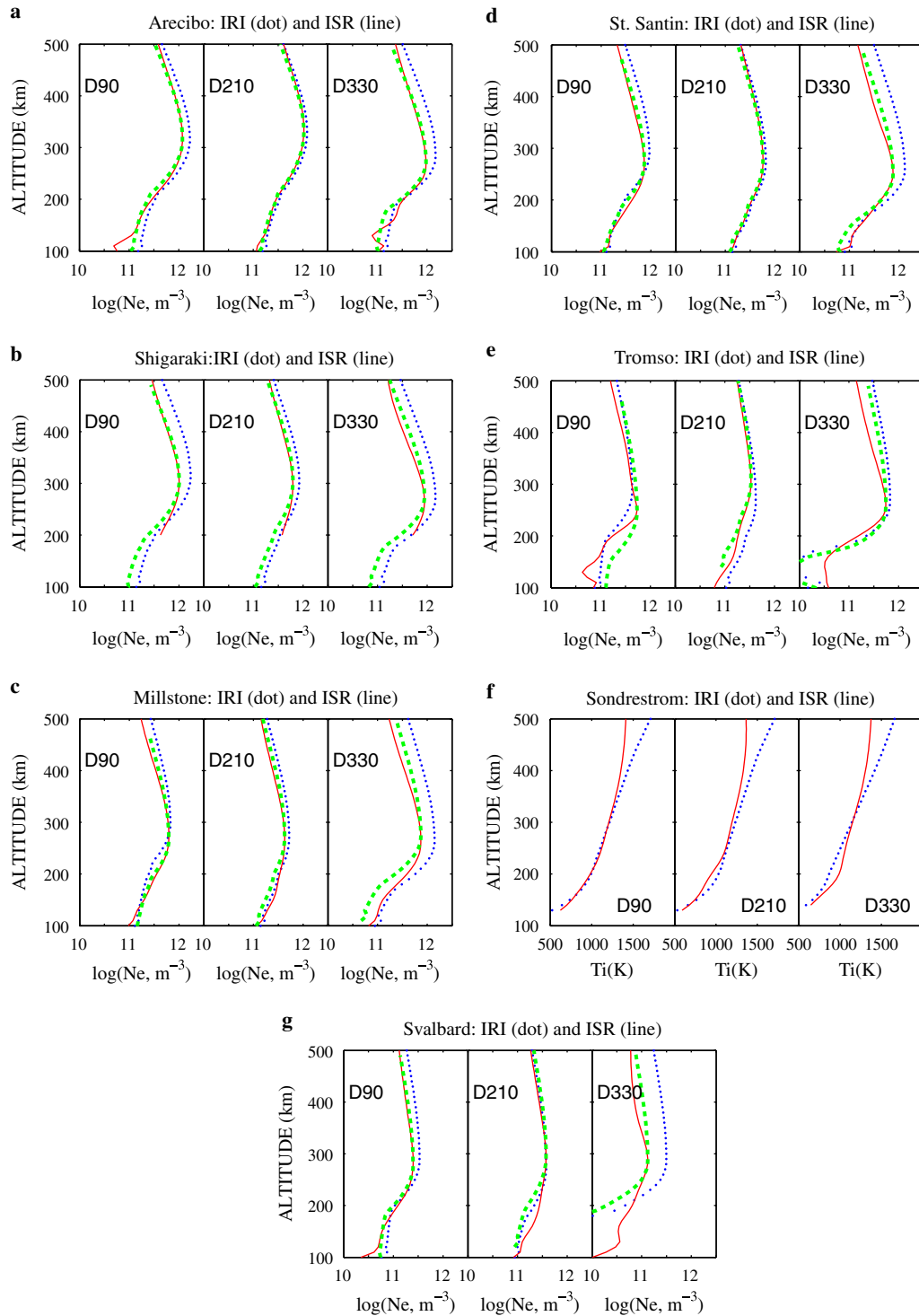


Fig. 2. Comparisons of Ne height variations between IRI (dots) and ISR (line) models for seven ISR sites at 1200 LT in spring (day number 90), summer (day number 210) and winter (day number 330). Shown also are the IRI profiles scaled to the ISR model for profile shape comparisons (thick dashed, see text). (a) Arecibo, (b) Shigaraki, (c) Millstone Hill, (d) St. Santin, (e) Tromso, (f) Sondrestrom, and (g) Svalbard.

maintains a small increase rate and it even decreases at the polar cap site.

3.3. Electron temperature

Fig. 4 shows Te comparisons between the ISR model and the two IRI options. Values from the two IRI Te mod-

els start to be separated at 450 km, and the Intercosmos data based IRI model tends to be slightly higher at high latitudes and lower at lower and middle latitudes than the corresponding Aeros/ISIS data based IRI model.

At low- or lower mid-latitudes, the height profile of daytime Te for median solar activity is characterized by non-monotonic variation, with a minimum at around the F2

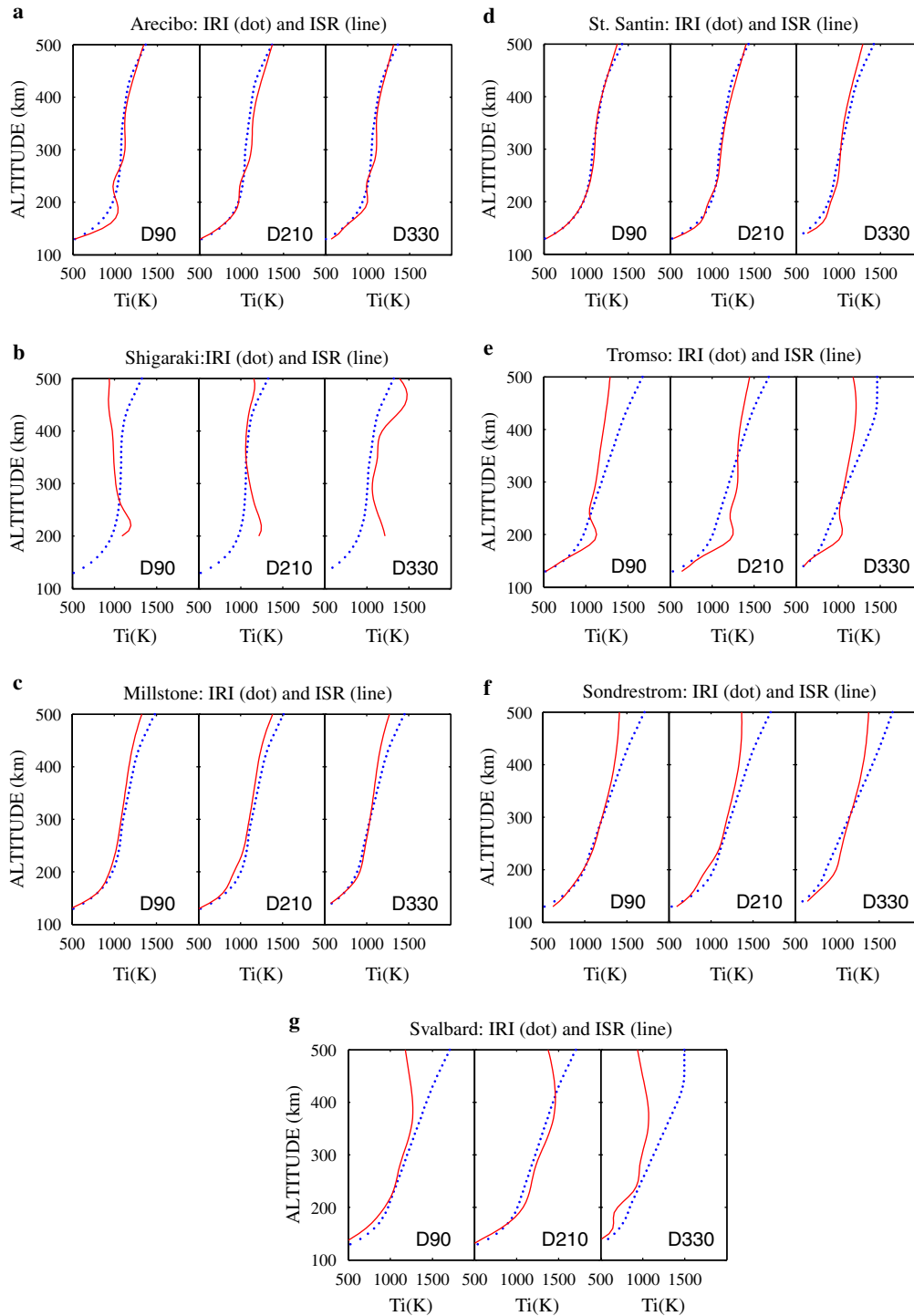


Fig. 3. Comparisons of Ti height variations between IRI (dots) and ISR (line) models for seven ISR sites at 1200 LT in spring (day number 90), summer (day number 210) and winter (day number 330). (a) Arecibo, (b) Shigaraki, (c) Millstone Hill, (d) St. Santin, (e) Tromso, (f) Sondrestrom, and (g) Svalbard.

peak or higher and an underlying bulge. Such a feature is captured by both models in spring and summer for Arecibo. In winter, it shows up in the ISR model but the IRI model sculpts a different variation with the bulge and minimum lying at higher altitudes. At Shigaraki, the ISR model could not do a good job of capturing the minimum in summer, and does not depict the bulge which occurs usu-

ally close to the low boundary of the quality data. As in Arecibo, in winter the ISR Te is lower than the IRI.

The minimum and bulge occurs at the mid-latitude site, St. Santin, in the ISR model but not in the IRI. Again, in winter, the ISR Te is lower from 200 to 400 km.

At Millstone Hill, in most cases the ISR Te is lower than the IRI. The difference becomes larger at higher altitude

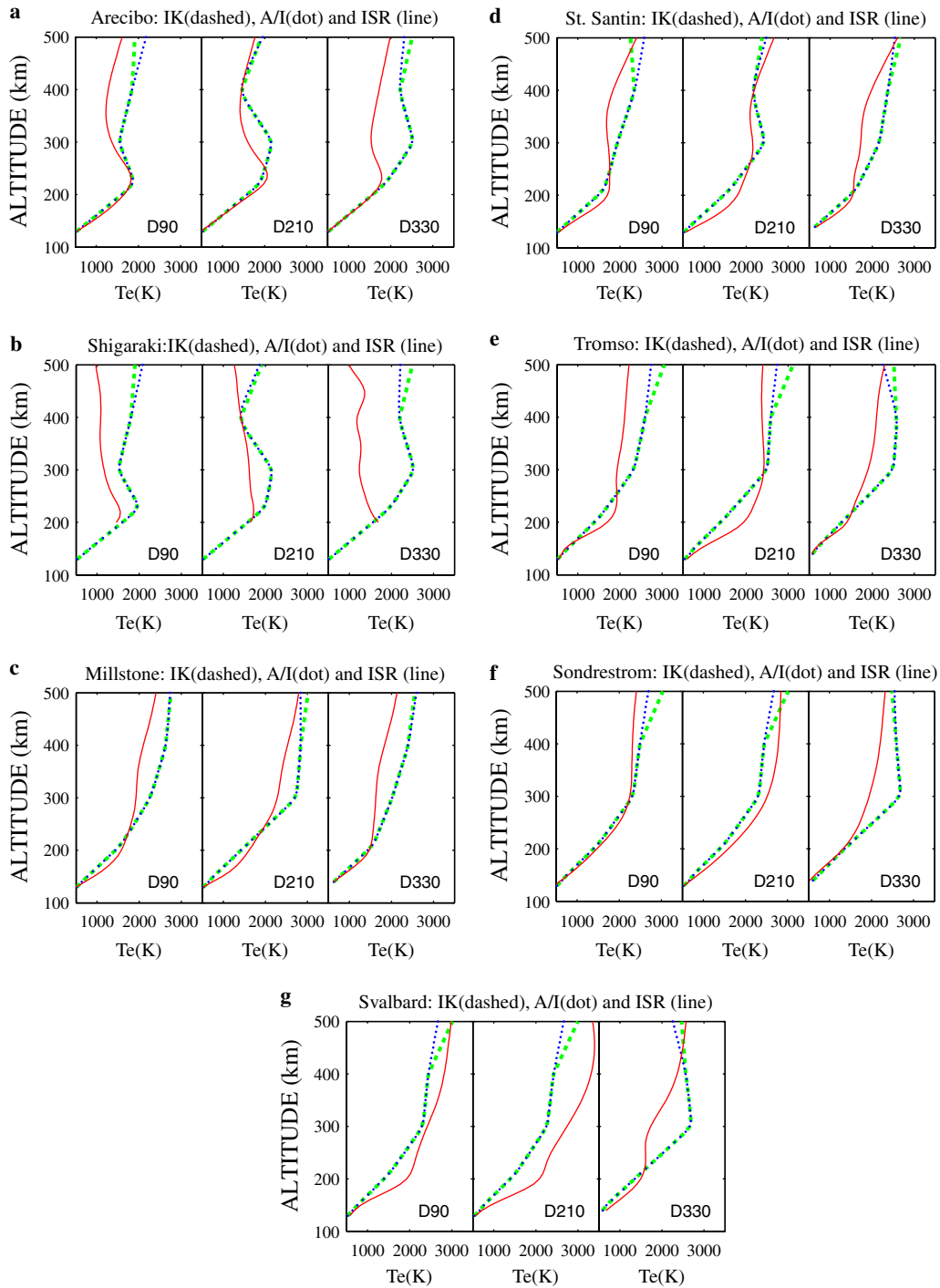


Fig. 4. Comparisons of Te height variations between IRI (dots for its standard model based on Aeros/ISIS data; thick dashed for the model based on Interkosmos) and ISR (line) models for seven ISR sites at 1200 LT in spring (day number 90), summer (day number 210) and winter (day number 330). (a) Arecibo, (b) Shigaraki, (c) Millstone Hill, (d) St. Santin, (e) Tromso, (f) Sondrestrom, and (g) Svalbard.

where Te is well separated from Ti and Tn. The difference is slightly smaller in summer.

At Tromsø, the models are more consistent in summer. At noon, the ISR Te tends to be lower in equinox and winter.

At Sondrestrom, agreement in equinox and summer is better at noon than in the afternoon when the IRI Te is lower. In winter, both models agree in the afternoon but

not at noon. For those high latitude sites, a common feature of the winter-time midday Te produced by the IRI is a maximum at about 300 km. This maximum, however, does not appear in the ISR model.

At Svalbard, the ISR Te is generally higher by up to 500 °K in equinox and summer than the IRI. As mentioned earlier, the relatively newer IRI Te model based on Interkosmos tends to give higher Te than the standard IRI

model based on Aeros/ISIS data, leading to slightly improved agreement with the ISR model.

The IRI model T_e is assumed to be solar activity independent. The ISR model assumes a linear dependence. Some of the difference discussed above may arise from the determination of solar activity dependency. A good approach taken to represent the dependence may rely on the selection of an appropriate solar flux index, as discussed in Bilitza et al. (2005) and Truhlik et al. (2005). It is also worthwhile to note that, as discussed in Zhang and Holt (2004) and Zhang et al. (2005a), such a dependence is a complicated one that is also related to the background Ne level. Perhaps, considering a solar index term with an electron density correction term would best address the solar cycle dependence of T_e .

4. Summary

Local empirical ionospheric models have been developed from long-term datasets of seven ISRs in American, European and Asian longitudes at Svalbard, Tromsø, Sondrestrom, Millstone Hill, St. Santin, Arecibo and Shigaraki. These models, as important complements to global models such as IRI, represent Ne, T_e , Ti and ion drifts in the E and F regions, giving a quantitative description of ionospheric properties.

We have reported a comparative study between the ISR local model and the IRI for median solar activity and quiet magnetic activity conditions. We have presented results for each of the seven ISR sites, focusing on height variations of Ne, Ti and T_e during the day in equinox, summer and winter seasons. Results of our comparisons can be summarized as follows:

- (1) For electron density, there is generally agreement between the two models in terms of the shape of the profile in the topside. In the bottomside, the ISR Ne model tends to give more F1 region ionization and a wider F region (or larger IRI B0 parameter). Agreement between the two models is better in equinox and summer than in winter, where the Ne decreases toward higher altitude at a rate higher for the ISR profile than for the IRI profile. At high latitudes in winter, while the IRI Ne is higher than the ISR Ne at the peak height and above, the ionization in the bottomside generated by the ISR model is higher as compared to the IRI model which indicates the absence of the E and lower F region ionization.
- (2) For Ti, good agreement between the two models prevails over most sites with Millstone Hill and St. Santin being excellent. Some larger differences occur at high altitudes for high latitudes, where the IRI Ti maintains a steady increase with height but the ISR Ti increases more slowly.
- (3) Variability in T_e due to solar activity, local time and season is usually larger than in Ti and Ne; thus, the

somewhat large difference between the two models are not totally surprising. Nevertheless, both models show the minimum and bulge on the T_e profile from low- and lower mid-latitudes, and generally a monotonic type of growth for subauroral and high-latitudes, however, the difference at noon seems larger in winter than in other seasons. In particular in winter at high latitudes, the IRI T_e , being higher than the ISR T_e , exhibits a maximum that does not exist in the ISR model.

The differences between the IRI and ISR models represent those between global and local models and are caused largely by smoothing procedures extensively applied to the global model. Meanwhile, the relatively worse agreement at high latitudes uncovers a basic fact that no significant amount of data has been taken into account by the IRI for high latitudes. This is perhaps most obvious for the plasma temperatures in the F region height. Long-term ISR datasets are indeed crucial ground-based data resources for the IRI improvement.

Acknowledgements

We thank the staff at EISCAT, Svalbard, Sondrestrom, and in particular, Bill Rideout and members of the Haystack Observatory Atmospheric Sciences Group for assembling and maintaining the Madrigal Database. We thank S. Kawamura for preparing the MU radar data. A. Zalucha and A. Brooks have been involved in model developments for St. Santin and Arecibo as REU students. This research was supported by NSF Space Weather Grant ATM-0207748 and NSF ATM-0417666. The Sondrestrom, Millstone Hill and Arecibo incoherent scatter radars are supported by the US National Science Foundation (NSF) as part of the Upper Atmosphere Facility program. EISCAT is an international association supported by the research councils of Finland (SA), France (CNRS), the Federal Republic of Germany (MPG), Japan (NIPR), Norway (NFR), Sweden (VR) and the United Kingdom (PPARC). The MU radar belongs to and is operated by the Research Institute for Sustainable Humanosphere of Kyoto University. St. Santin and Arecibo data were imported from the CEDAR database. The IRI model was obtained from NASA's Space Physics Data Facility.

References

- Bilitza, D. International Reference Ionosphere 2000. *Radio Sci.* 36, 261–275, 2001.
- Bilitza, D. A correction for the IRI topside electron density model based on Alouette/ISIS topside sounder data. *Adv. Space Res.* 33 (6), 838–843, 2004.
- Bilitza, D., Radicella, S.M., Reinisch, B.W., Adeniyi, J.O., Mosert Gonzalez, M.E., Zhang, S.R., Obrou, O. New B0 and B1 models for IRI. *Adv. Space Res.* 25 (1), 89–95, 2000.

- Bilitza, D., Williamson, R. Towards a better representation of the IRI topside based on ISIS and Alouette data. *Adv. Space Res.* 25 (1), 149–152, 2000.
- Bilitza, D., Richards, P., Truhlik, V., Abe, T., Triskova, L. Solar Cycle Variations of Topside Electron Density and Temperature: Altitudinal, Latitudinal, and Seasonal Differences, IRI 2005 Workshop, Roquetes, Spain, 27 June–1 July 2005.
- Doe, R.A., Thayer, J.P., Solomon, S.C. Incoherent scatter radar measurements and modeling of high-latitude solar photoionization. *J. Geophys. Res.* 110, A10303, doi:10.1029/2005JA011129, 2005.
- Holt, J.M., Zhang S.-R., Buonsanto, M.J. Regional and Local Ionospheric Models Based on Millstone Hill Incoherent Scatter Radar Data, *Geophys. Res. Lett.*, 29, doi: 0.1029/2001GL013579, 2002.
- Truhlik, V., Bilitza, D., Triskova, L. Evaluation of indices for description of solar activity dependence of the electron temperature and density in the topside ionosphere, IRI 2005 Workshop, Roquetes, Spain, 27 June–1 July 2005.
- Zhang, S.-R., Holt, J.M. Ionospheric temperature variations during 1976–2001 over Millstone Hill. *Adv. Space Res.* 33, 963–969, doi:10.1016/j.asr.2003.07.01, 2004.
- Zhang, S.-R., Holt, J.M., Zaluca, A.M., Amory-Mazaudier, C. Mid-latitude ionospheric plasma temperature climatology and empirical model based on Saint Santin incoherent scatter radar data from 1966–1987. *J. Geophys. Res.* 109, A11311, doi:10.1029/2004JA010709, 2005a.
- Zhang, S.-R., Holt, J.M., van Eyken, A.P., McCready, M., Amory-Mazaudier, C., Fukao, S., Sulzer, M. Ionospheric local model and climatology from long-term databases of multiple incoherent scatter radars. *Geophys. Res. Lett.* 32, L20102, doi:10.1029/2005GL023603, 2005b.